

Two-dimensional Continuous Extraction in Multiphase Lipid Bilayers to Separate, Enrich, and Sort Membrane-bound Species

*Ling Chao†+, Mark J. Richards†, Chih-Yun Hsia, and Susan Daniel**

School of Chemical and Biomolecular Engineering, Cornell University, Ithaca, NY.

*Correspondence should be addressed to S.D. (sd386@cornell.edu).

SUPPORTING INFORMATION

Contained herein are details on materials and suppliers, experimental setup and procedures, microfluidic device fabrication, supported bilayer preparation, system characterization, control experiments, and a movie to illustrate separation and sorting in the microfluidic device.

MATERIALS, EXPERIMENTAL SETUP, AND METHODS

Materials. 1-Palmitoyl-2-oleoyl-sn-glycero-3-phosphocholine (POPC), Ovine wool cholesterol (Chol), 18:0 N-palmitoyl-D-*erythro*-sphingosylphosphorylcholine (PSM) were purchased from Avanti Polar Lipids (Alabaster, AL). N-(4,4-difluoro-5,7-dimethyl-4-bora-3a,4a-diaza-s-indacene-3-propionyl)-1,2-dihexadecanoyl-sn-glycero-3-phosphoethanolamine, triethylammonium salt (head-labeled BODIPY FL DHPE), and Alexa Fluor 594 hydrazide used to label the head group of asialoganglioside-G_{M1} were purchased from Invitrogen (Eugene, OR). Bovine brain asialoganglioside-G_{M1} and all other reagents, unless otherwise specified, were purchased from Sigma (St. Louis, MO). Glass coverslips (25 mm x 25 mm; No. 1.5) from VWR

were used as solid supports for the bilayers. Polydimethylsiloxane (PDMS; Sylgard 184) polymer used to fabricate microfluidic devices was purchased from Robert McKeown Company (Branchburg, NJ).

Fluorescence microscopy. Images were obtained using an inverted Zeiss Axiovert Observer.Z1 fluorescence microscope equipped with α Plan-Apochromat objectives, a Hamamatsu EM-CCD camera (ImageEM, model C9100-13, Bridgewater, NJ), and X-Cite® 120 microscope light source (Lumen Dynamics Group Inc., Canada). ET GFP filter cube (49002, c106273, Chromatech Inc.) was used to collect the fluorescence emitted from BODIPY fluorophores. ET MCH/TR filter cube (49008, c106274, Chromatech Inc.) was used to collect the fluorescence emitted from Alexa 594 fluorophores.

Zeiss AxioVision software was used to obtain images and the fluorescence intensity data for lipid diffusion and separation analyses. The contrast of an entire image was enhanced in ImageJ (NIH, Bethesda, MD) when necessary.

Preparation of lipid vesicles for formation of supported lipid bilayers. Lipids dissolved in a methanol and chloroform solution were mixed together at the desired compositions and then dried under a vacuum desiccator to remove the solvent. The dried lipid mixture was then reconstituted into multi-lamellar vesicles at a concentration of 2 mg/ml in buffer composed of 5 mM phosphate buffered saline (PBS) with 150 mM NaCl at a pH of 7.4. LUVs were formed by extruding the reconstituted mixture 19 times through a 50 nm Whatman polycarbonate filter in an Avanti Mini-Extruder (Alabaster, AL). The vesicle solutions were diluted to 0.5 mg/mL before use. All vesicles were on the order of 100 nm in diameter after processing as determined by dynamic light scattering measurements (Zetasizer Nano, Malvern Instruments, Worcestershire, UK).

Microfluidic channel preparation. The polydimethylsiloxane (PDMS) microfluidic device was made by standard soft-lithography procedures at the Cornell Nanoscale Facility. PDMS prepolymer, along with a curing agent, was cast on the silicon wafer mold and cured at 85°C for 3 hrs, producing a soft flexible material with the channels embedded in negative relief once removed from the mold. The channel inlets and outlets are connected to outside tubing by punching the PDMS mold with 20 gauge needles (610 μm ID). Glass coverslips, which become the fourth wall of the microfluidic channel, were cleaned in piranha solution (70:30 volume ratio of H_2SO_4 to 50% H_2O_2) for 10 min and rinsed thoroughly with distilled water for 20 min. Before use, glass slides and the PDMS mold were rinsed with deionized water, dried under high purity nitrogen air, and then treated with oxygen plasma using a Harrick Plasma Cleaner (Model # PDC-32G, Ithaca, NY) at a pressure of 750 micron on the high setting for 30 seconds. Immediately after plasma cleaning, the glass slide and PDMS mold were pressed together and heated for 10 minutes at 80°C to seal the microfluidic channel device.

Formation of patterned supported lipid bilayers in a single stage microfluidic device. In this work, SLBs are formed during laminar flow conditions instead of under stagnant incubation. Laminar flow is advantageous for patterning heterogeneous bilayers in microfluidic channels because particles follow streamlines with minimal mixing¹. Thus, lipid vesicles of different compositions can be sent through the channel on different streamlines and upon rupture will form contiguous, parallel bilayers. If the compositions are chosen so that they are phase stable, these bilayer stripes will have stable interfaces. The compositions of the two coexistent phases used in this work were chosen based on a published ternary phase diagram of POPC/PSM/Chol^{2,3}. We plotted a hypothetical tie line in this phase diagram, guided by previous literature^{3,4} and chose phase compositions close to the ends of this tie line. Recent work corroborates our

selection of compositions for two-phase stability⁵. These compositions are 70/20/10 molar ratio of POPC/PSM/Chol, denoted as l_d phase, and 60/40 molar ratio of PSM/Chol, denoted as l_o phase. We found that we could pattern a composite membrane based on these compositions inside a microfluidic channel using laminar flow (as will be described in detail next) to define regions of specific lipid phases within the channel. Membrane-bound biomolecules are able to move between the phases after patterning.

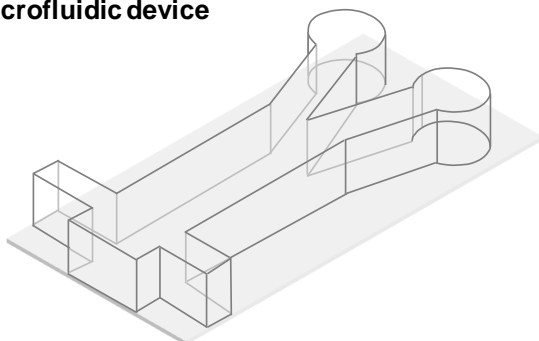
To form a composite lipid bilayer with these lipid phases and load membrane at specified locations, we used the following procedure illustrated in Fig. S1. First, we sent l_o phase vesicles and a buffer stream concurrently through the main microfluidic channel. The buffer flow serves to keep the l_o phase vesicle stream, and thus the supported l_o phase bilayer, confined to one side of the channel. During this step, the system was heated to 65°C (both the device and the lipid mixture), so that the l_o phase lipid mixture was above its phase transition temperature and readily fused to the glass surface to form a bilayer. Afterwards, a 65°C buffer was used to rinse out the excess vesicles and the system was equilibrated to room temperature for 1 hr to allow the l_o phase membrane to gradually cool down. Next, the vesicles with load mixture (mixture denoted as red and green dots in orange background) were sent through the perpendicular loading channel. The load mixture was composed of the same composition as lipid l_d phase, but also included small amounts of the labeled glycolipid, Alexa 594-G_{M1}, and BODIPY DHPE lipid (approx. 1 mol% of each). At the same time, buffer flow from all other ports was maintained at a slow rate to prevent the load vesicles from entering into the main channel (these streams are omitted in the illustration). The membrane with the load mixture formed only on the glass surface where there was no bilayer under the stream of the load vesicles. Finally, l_d phase

vesicles were sent through the main channel (denoted as a pink arrow in the figure) and filled the exposed regions of the glass surface that had not been covered by lipid membranes.

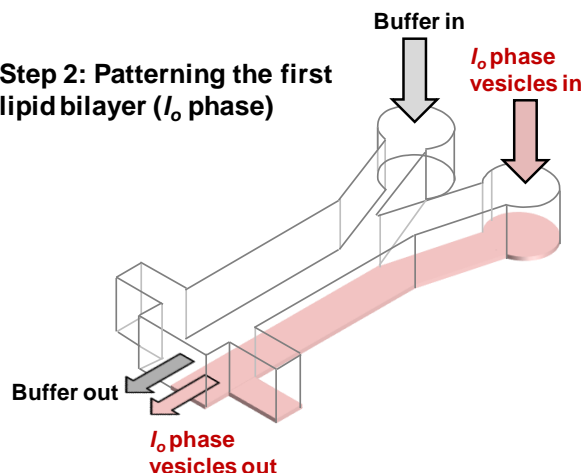
In all of these steps, vesicles were exposed to the glass surface for 5 min under flow and then rinsed with buffer for 20 min. When the load formed, the flow rate of the load vesicle solution in the upstream side channel (50 μm wide and 70 μm high) was 10 $\mu\text{L}/\text{min}$ and the overall flow rate of the load vesicle solution and buffers in the downstream side channel (50 μm wide and 70 μm high) was 30 $\mu\text{L}/\text{min}$. When the lipid phases formed, the flow rates of vesicle solutions and rinsing buffers were kept at 20 $\mu\text{L}/\text{min}$ in the main channel (100 μm wide and 70 μm high).

To transport the mixed species into the main composite bilayer channel after bilayer formation, aqueous buffer flow was applied in the main channel towards the “Y” branch into the exit ports at a rate of 80 $\mu\text{L}/\text{min}$. The hydrodynamic flow provided a shear force on the membrane biomolecules that served to drag them along the main channel. Biomolecules were able to partition into either membrane phase across the channel by diffusion and were collected at the end of the channel in the separate ports.

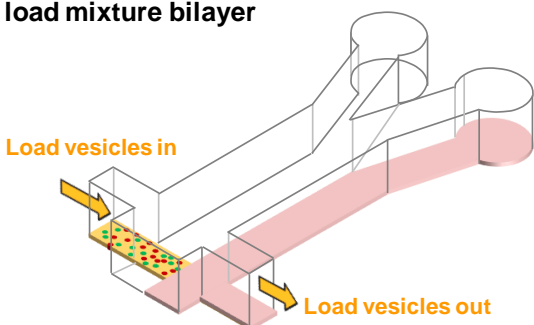
Step 1: Unpatterned microfluidic device



Step 2: Patterning the first lipid bilayer (l_o phase)



Step 3: Patterning the load mixture bilayer



- l_d phase preferring species
- l_o phase preferring species

Step 4: Patterning the second lipid bilayer (l_d phase)

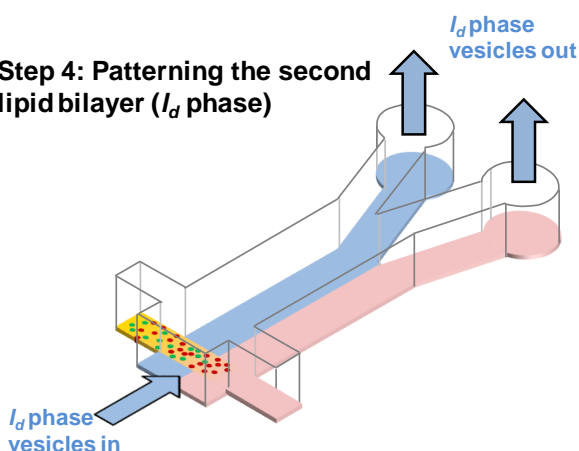


Figure S1. A three dimensional cut away view illustrating the loading and patterning of bilayers into the microfluidic device via vesicle fusion and laminar flow patterning, as described in the text. The pink color represents lipid l_o phase, the lipid-ordered bilayer; the blue color represents lipid l_d phase, the lipid-disordered bilayer; and the orange color represents the load bilayer that is the same composition as l_d phase, except that it contains the biomolecules to be separated and sorted. Green and red circles represent the biomolecule mixture. The arrows show the direction of the flow and streamlines as the pattern is being formed. Step 1: the blank microfluidic device design consisting of a clear PDMS mold bound to a glass support. The glass support is removed in the subsequent illustrations for clarity. Step 2: patterning lipid l_o phase. During this step the device is warmed to $\sim 65^\circ\text{C}$. Step 3: forming the load bilayer containing the mixture of membrane-bound biomolecules after l_o phase bilayer has been formed. Load only forms where vesicles contact glass, i.e. not where l_o phase bilayer already exists. Buffer flow also enters from the sides to confine the flow to the loading channel, but is omitted here for clarity. Step 4: patterning the l_d phase bilayer after both the load and l_o phase bilayers are formed. Note that while the l_d phase bilayer is forming, some of the l_o phase-prefering species (red here) begin to partition into the l_o phase bilayer adjacent to the mixture load.

SYSTEM CHARACTERIZATION

Characterization of the stability of the patterned bilayers. To ensure the extraction we observed was not an artifact of the patterning procedure, we ran the following control, summarized in Fig. S2. We patterned a two-phase stable bilayer with load bilayer (l_d phase) in one half of the channel and l_o phase bilayer in the other half. After four hours it is clear that l_o phase is enriched in Alexa 594- G_{M1} and l_d phase is enriched in BODIPY DHPE. A second device was patterned with load bilayer in one half of the channel and l_d phase in the other half. After four hours the channel was completely uniformly mixed, no interface was present between patterned bilayers, and the location of Alexa 594- G_{M1} could not be distinguished from the BODIPY DHPE.

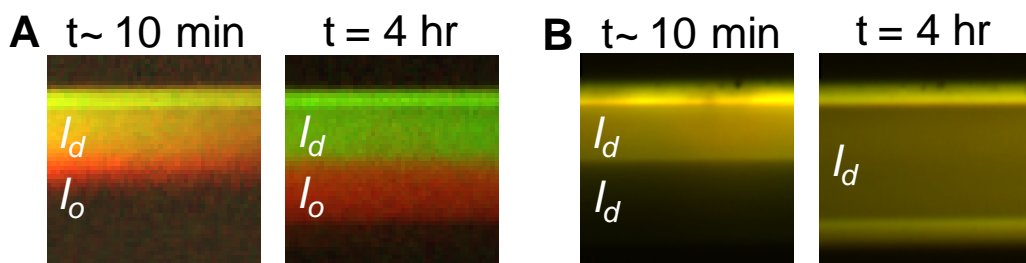


Figure S2. Stability of patterned membranes inside the microfluidic channel. The dimension of the channel (width, top to bottom in image) is 100 μm . (A) Two-phase coexistent compositions: the membrane in the top half of the channel (yellow color) contains l_d phase bilayer doped with a mixture of 1 mol% green BODIPY DHPE and 1 mol% red Alex 594- G_{M1} at time = 0. The membrane in the bottom half of the same channel contains l_o phase bilayer with no fluorophores in it initially. The leftmost panel is the image taken 10 min after the membrane was prepared, after some partitioning has commenced between the phases. Alex 594- G_{M1} favors the l_o phase bilayer and its enrichment is apparent by the red color in the lower half of the channel after 10 min. BODIPY-head (green) prefers the l_d phase bilayer and remains there. After about four hours, the interface between the two phases based on the fluorescence intensity of the two fluorophores can still be clearly observed, indicating that the phase separation is stable. (B) l_d phase composition only: the membrane in the top half of the channel contains l_d phase bilayer doped with 1 mol% BODIPY-head and 1 mol% Alexa 594- G_{M1} as in (A); however, the membrane in the bottom half contains the same membrane composition (l_d phase) with no fluorophores initially. At ten minutes and four hours after formation of the supported bilayers, no preference for either biomolecule for either region was observed and no interface between the two regions was observed even after four hours (the bilayers became fully mixed). The entire channel width is 100 μm .

Additionally, we characterized the interface stability under flow conditions. Using fluorescence profiles at the center of the channel to determine the interface location during an extraction run we found that the interface locations do not change after 3 hrs of buffer flow, and then after an additional 5 hrs, as shown in Fig S3.

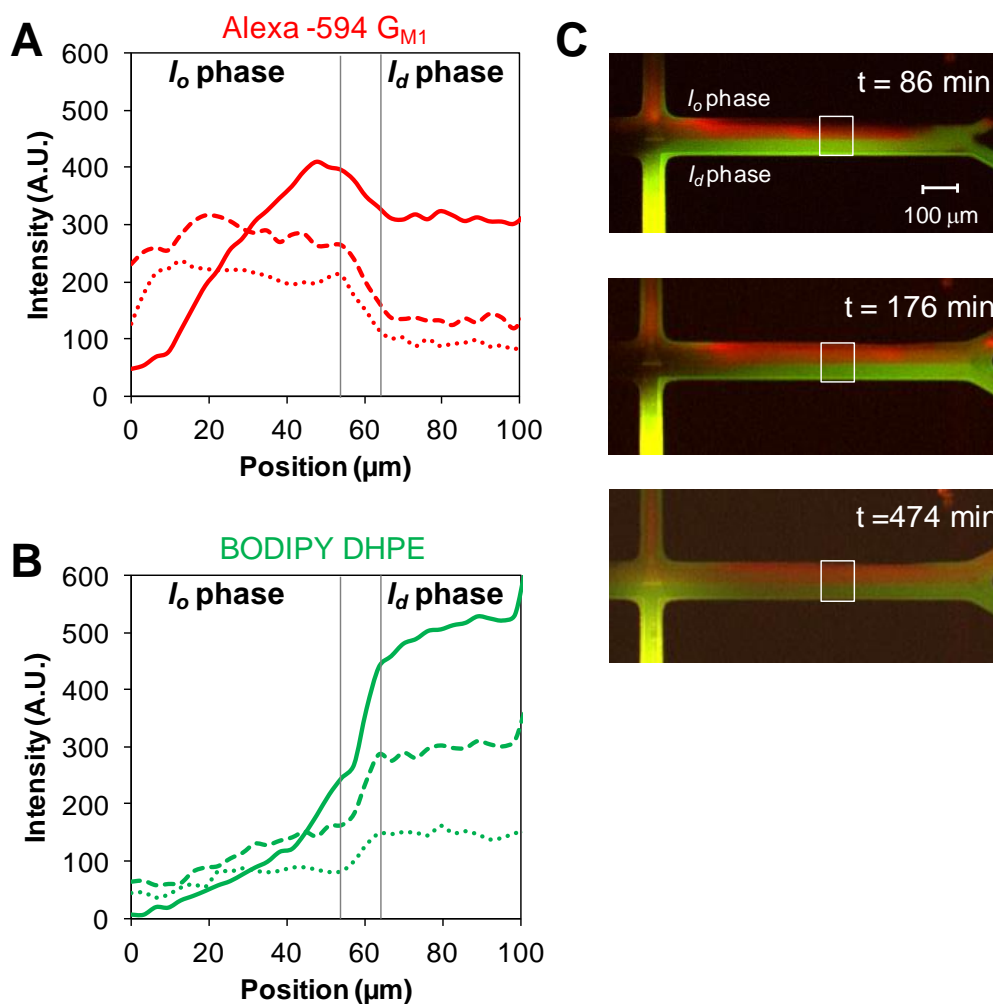


Fig. S3. Fluorescence intensity profiles across the extraction channel for various time points. (A) Alexa 594- G_{M1} (red) and (B) BODIPY DHPE (green) both indicate a stable $\sim 10\mu\text{m}$ interface throughout this experiment. The interface edges (marked with vertical gray lines) are defined as the locations where species intensities noticeably drop off. Here we show three time points to illustrate how the interface edges were defined. (C) In this experiment, $80\ \mu\text{l}/\text{min}$ of bulk flow was applied in the microfluidic channel for 3 hours then stopped and the device monitored for an additional 5 hours. The solid lines indicate concentration across the channel at an early stage of experiment ($t = 86\ \text{min}$); the dashed lines correspond to 3 hours after starting the experiment with flow ($t = 176\ \text{min}$); and dotted lines correspond to concentration across the channel 5 hours after flow was stopped ($t = 474\ \text{min}$).

Background removal and vignetting correction. A background subtraction was used to reduce the effect of fluctuations in the light source and to zero the baseline measurement. Background levels measured immediately adjacent to the channel at each time point were subtracted from all intensity measurements. Even after background subtractions, we found that vignetting remained an issue in our system such that our mass balance did not close entirely. Vignetting causes intensities in the center of the image to be slightly higher than at the edges. The main effect of this on our mass balance is to cause the inlet and outlet fluxes to differ depending on where they were located relative to the center of the field of view.

To correct for slight variation in light intensity, we applied a vignetting correction factor (f) to scale the outlet intensity to account for slight uneven illumination. We used the mass balance to solve for this factor at various positions, L , along the channel then fit the data to a second order polynomial $F(x)$ which could then be used to scale the intensity at any position in the channel. We found that less than 10% correction was required to correct for uneven illumination. The vignetting correction was performed for BODIPY DHPE and Alexa 594-GM₁ independently.

Characterization of diffusion in supported lipid bilayer by Fluorescence Recovery After Photobleaching (FRAP). To measure the diffusion coefficient of species in the supported bilayer, a 20 μm diameter spot in the supported lipid bilayer was bleached with a 4.7 mW wavelength tunable Argon/Krypton laser (CVI Melles Griot, Model 643-AP-A01) for 200 ms at the appropriate wavelength for each fluorophore label. The recovery of the fluorescence intensity of the photobleached spot was recorded for 15 minutes. Each image was background subtracted and normalized. The recovery data was fit using a Bessel function following the method of

Soumpasis⁶. The diffusion coefficient was then calculated using the following equation:

$$D = \frac{w^2}{4t_{1/2}},$$
 where w is the width at half-maximum of the Gaussian profile of the focused beam.

Characterization of the velocity profile in a two-phase supported bilayer using fluorophore photobleaching. In order to visualize and determine the velocity profile within the two-phase striped bilayer, a photobleaching technique was performed similar to that described by Jönsson et al⁷. Briefly, the convective motion of the SLB containing fluorescent species was driven by shear force, provided by the flow of buffer through the microfluidic channel. Flow was started prior to the bleaching experiment to ensure a fully-developed flow profile at a rate of 80 $\mu\text{L}/\text{min}$ in the main channel. A thin photobleached line was created across the channel width on the SLB under a 20x objective with an Argon-Krypton tunable laser. The photobleached line was generated by quickly moving the stage relative to the focused, stationary laser spot. Images were recorded every 10 seconds post bleach. The photobleached band moved along the direction of the flow and its shape changed accordingly as shown in Fig. 3 in the main text. The displacement of the photobleached line along with its shape evolution reveals how the target molecules are transported in the SLB and was used to determine a model for the velocity profile in the two-phase bilayer. In this experiment both phases of the bilayer were doped with 1 mol% BODIPY DHPE so that the entire cross-section of the bilayer could be photobleached with a single laser line and tracked.

The velocity profile in a homogeneous bilayer induced by hydrodynamic flow at the bilayer surface within a rectangular channel (Fig. 2B *main text*) is described by the following set of equations^{8,9}:

$$\sigma_{hydro}(y) = -\frac{\Delta p}{\Delta x} \frac{h}{2} \left(1 - \frac{8}{\pi^2} \sum_{k_{odd}} \frac{1}{k^2} \frac{\cosh\left(\frac{k\pi y}{h}\right)}{\cosh\left(\frac{k\pi w}{h}\right)} \right) \quad (\text{Eq. S1})$$

$$v(y) = \frac{\sigma_{hydro}(y)}{b} e_x \quad (\text{Eq. S2})$$

where $\sigma_{hydro}(y)$ is the shear force from hydrodynamic bulk fluid flow; $\Delta p/\Delta x$ is the pressure drop over length of the channel; y is the position across the channel, perpendicular to the flow direction; h is the channel height; $2w$ is the width of channel; $v(y)$ is the velocity; b is the intermonolayer friction factor; and e_x is the unit vector in the x direction. Note here that the buffer flow is assumed to be fully developed and constant and that viscous forces and surface pressure gradients are negligible compared to the hydrodynamic force⁹. This equation for the bilayer velocity was the basis of each part of our piecewise model (Eq. 5 *main text*).

MODEL EVALUATION

A simple model of the extraction channel was developed which used experimental concentration data and measured quantities to predict the species distribution during an extraction run (Fig. S4).

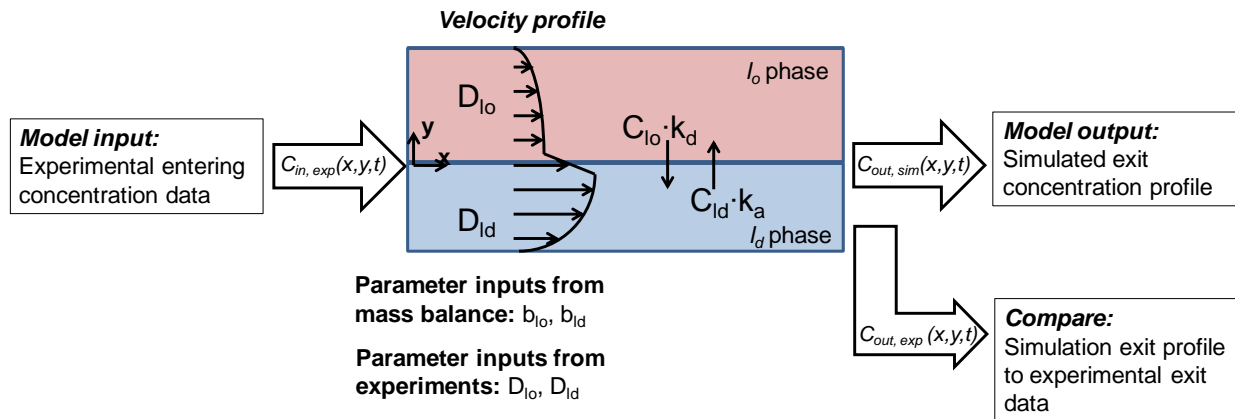


Figure S4. Strategy for comparing experimental data to simulated concentration profiles from the COMSOL model of convection-diffusion.

The model governing equation comes from the convection-diffusion process with an imposed velocity profile in the x-direction, given by the following equation:

$$\frac{\partial c(x, y, t)}{\partial t} = \nabla(D(y)\nabla c(x, y, t)) - \nabla(\vec{v}(y)c(x, y, t)) \quad (\text{Eq. S3})$$

where c is the concentration of the species, D is the diffusion coefficient of a species, and v is the velocity of the species. The diffusivity of each species in each phase is experimentally measured and is dictated by the properties of the lipid environment. We used fluorescence recovery after photobleaching to determine diffusion coefficients of each species in separate experiments (as described above). These values are reported in Table S1.

Table S1. Diffusion coefficient values used in Eq. 14 in the COMSOL simulation.

Lipid environment	BODIPY DHPE	G_{M1}
Liquid-ordered phase	0.63 $\mu\text{m}^2/\text{s}$	0.70 $\mu\text{m}^2/\text{s}$
Liquid-disordered phase	0.13 $\mu\text{m}^2/\text{s}$	0.14 $\mu\text{m}^2/\text{s}$

The velocity profile assumed here is that given by Eq. 5 (*main text*). Note that the experimentally measured inlet concentrations from raw fluorescence intensity values are the inputs to the COMSOL model. The boundary condition at the interface between phases is a flux corresponding to the partitioning kinetics of the system:

$$\frac{dN_{l_o}(x, t)}{dt} = k_a c_{l_d}(x, t) - k_d c_{l_o}(x, t) \quad (\text{Eq. S4})$$

In this equation, N is the accumulation in the liquid-ordered phase, c represents concentration at the interface in either the l_d or l_o phases, and k_a and k_d represent the association and dissociation rate constants for the l_o phase, respectively.

The model was evaluated by comparing predicted outlet concentration profiles with experimentally measured profiles. Figure S5 shows comparisons of predicted to measured profiles for both G_{M1} (red) and BODIPY DHPE at the three different channel lengths studied. The parameters used in these cases were measured diffusivities and partitioning coefficients and calculated intermonolayer friction factors (see Eq. 7 *main text*). It was found that these parameters resulted in close matches to experimental data, especially for the shorter channel lengths. Increasing the friction factor would lead to a later eluting plug and decreasing leads to an earlier eluting plug causing significant mismatch in the profiles.

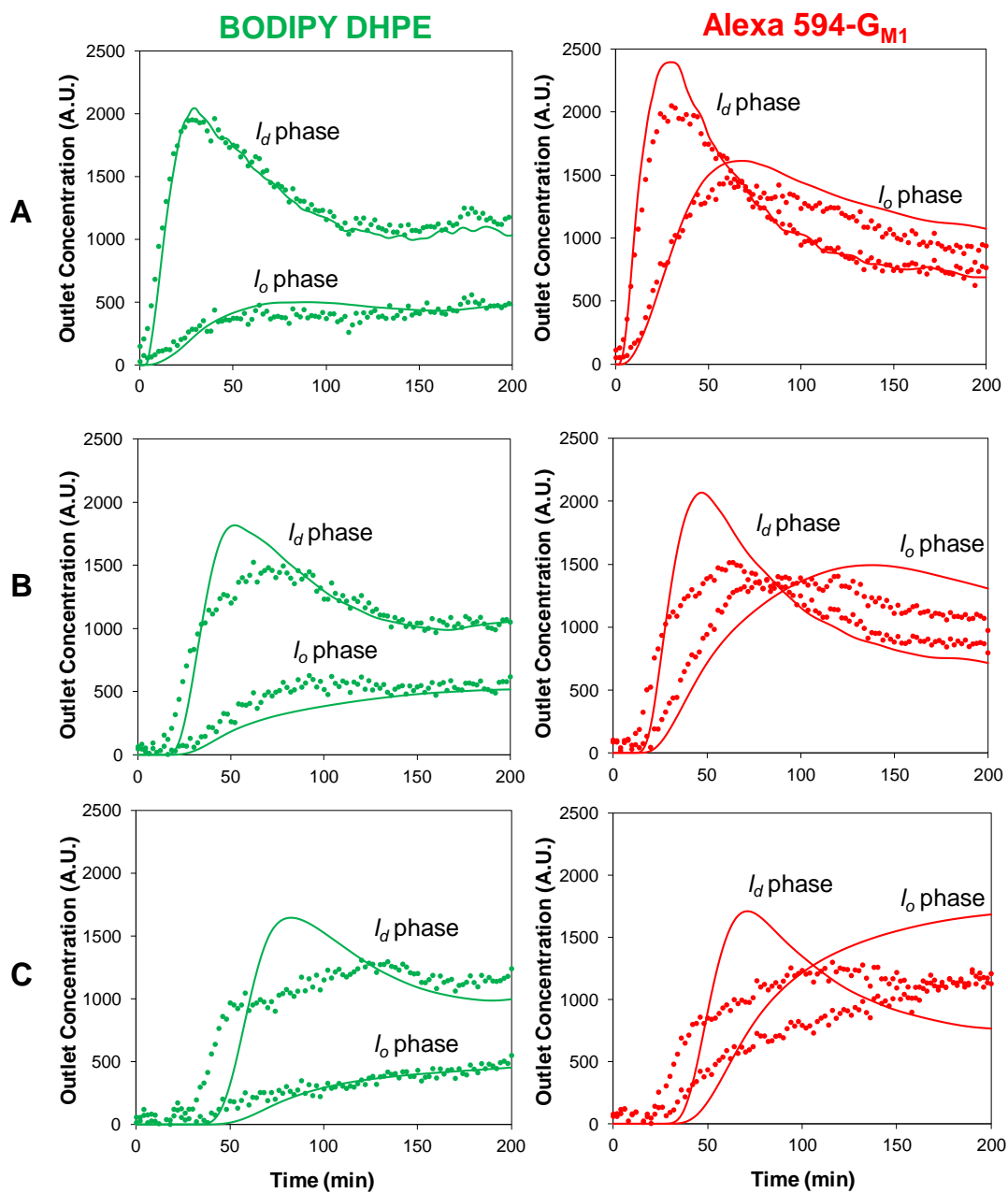


Figure S5. Comparison of outlet concentrations in each lipid phase from a representative experiment (points) to model predictions (solid lines) for various channel lengths. (A) 89 μm ; (B) 355 μm ; (C) 710 μm . Data are separated into average *l_o* and *l_d* phase concentrations in the control volume for BODIPY DHPE (green, left side) and Alexa 594-G_{M1} (red, right side).

There are some differences between the predicted concentration profiles and the experimentally measured profiles that we attribute to complexities not accounted for in this model. We believe one source could be patterning and bilayer imperfections. Our model assumes that the geometry of the bilayer phases is two rectangular regions, but imperfections in the patterning could lead to varied extractor geometries. Additionally, minor bilayer imperfections in the extractor contribute to a dispersive effect in part by immobilization of species in bilayer defects. The cumulative effect of these defects could lead to deviations between the model predictions and the fluorescence data over long channel lengths. Dispersion differences are apparent by the change in the shape of the experimental data compared to the simulation curve as the channel length increases. Notice that the peak position for the experimental data and simulation generally remain registered, which is most obvious in the l_d phase data, but as the channel length increases, the width of the experimental peak grows larger relative to the simulation. In addition, we have made the simplifying assumption in our model that the interface region is infinitesimally small. Perhaps modeling the interface region as having a finite width with mixed phase properties could also improve the accuracy of the simulation.

CONTROL EXPERIMENTS

Control experiment conducted in single phase bilayer. The following control experiment shows that the observed enrichment of species along the axial length of the channel is not an artifact of the experiment. Here we conduct the experiment in exactly the same manner as described previously, except that instead of patterning with a two-phase bilayer of parallel phase zones down the axial length of the channel, we pattern the channel with a bilayer of only one composition (l_d phase). In Fig. S6, l_d phase has been patterned in the channel and illustrates that

enrichment is not observed in the absence of a two-phase patterned bilayer. A similar result is obtained when only l_o phase bilayer is used as a homogenous bilayer phase in the channel.

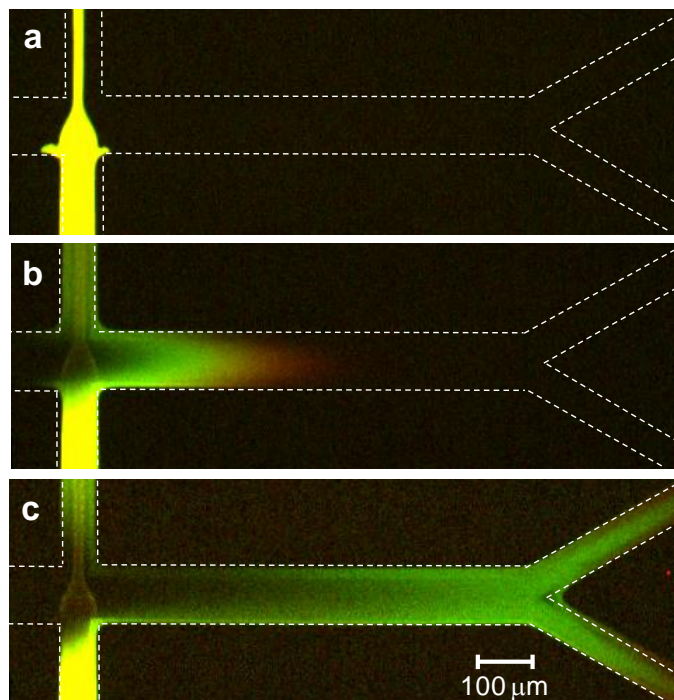


Figure S6. Control experiment of separation channel composed of only one phase. In this case only l_d phase composition is used to pattern the microchannel with a bilayer. In (a) the load consists of a mixture of Alexa 594- G_{M1} (red) and BODIPY DHPE (green). The dashed lines are superimposed on the image to outline the microchannel. (b) The load channel is transported down the main microchannel by hydrodynamic flow and no partitioning across the channel is observed. (c) In the absence of the two-phase bilayer, equal portions of the initial load are split equally at the “Y”, resulting in no separation, sorting, or concentration of species from the initial load amount.

SORTING MOVIE

1. Separation and sorting of Alexa 594- G_{M1} and BODIPY DHPE in a patterned, two-phase bilayer. The movie has been sped up to play at 4 frames/sec, while the interval between each frame in the actual experiment is 2 min.

REFERENCES

- (1) Kam, L.; Boxer, S. G. *J. Am. Chem. Soc.* **2000**, *122*, 12901.
- (2) Veatch, S. L.; Keller, S. L. *Phys. Rev. Lett.* **2005**, *94*, 148101.
- (3) Veatch, S. L.; Gawrisch, K.; Keller, S. L. *Biophys. J.* **2006**, *90*, 4428.
- (4) Veatch, S. L.; Polozov, I. V.; Gawrisch, K.; Keller, S. L. *Biophys. J.* **2004**, *86*, 2910.
- (5) Ionova, Irina V.; Livshits, Vsevolod A.; Marsh, D. *Biophys. J.* **2012**, *102*, 1856.
- (6) Soumpasis, D. M. *Biophys. J.* **1983**, *41*, 95.
- (7) Jönsson, P.; Höök, F. *Langmuir* **2011**, *27*, 1430.
- (8) Jönsson, P.; Höök, F. *Langmuir* **2010**, *27*, 1430.
- (9) Jönsson, P.; Beech, J. P.; Tegenfeldt, J. O.; Höök, F. *Langmuir* **2009**, *25*, 6279.